Patterns under quantum confined Stark effect

1998 J. Phys.: Condens. Matter 10 L539

(http://iopscience.iop.org/0953-8984/10/31/003)

J. Phys.: Condens. Matter **10** (1998) L539–L546. Printed in the UK PII: S0953-8984(98)94724-5

LETTER TO THE EDITOR

Patterns under quantum confined Stark effect

L L Bonilla, V A Kochelap† and C A Velasco‡

Universidad Carlos III de Madrid, Escuela Politécnica Superior, Butarque 15, E-28911 Leganés, Spain

Received 1 June 1998

Abstract. We have studied pattern formation under the quantum confined Stark effect and found different patterns with complex structure of the electron and hole wave functions which give rise to nonuniform dipolar patterns of the electric charge inside the quantum well layer. The results obtained indicate spontaneous breaking of the transversal invariance, which can lead to new optical effects and transport phenomena.

The quantum confined Stark effect (QCSE) [1] arises when a strong electric field is applied to a quantum well (QW) heterostructure. This field affects the energies and wave functions of electron and hole subbands, as well as exciton states. Because of the underlying physics, the QCSE is highly sensitive to the photo-generation of electrons and holes. Electrons and holes screen the applied field and produce considerable changes in the optical spectra near the fundamental edge of absorption. These spectra become dependent on the concentration of the electron–hole plasma, i.e., on the intensity of illumination. Moreover, if the spectrum of the illuminating light is tuned into the region between exciton and interband absorption, the QCSE becomes an example of the nonlinear electro-optical effect in its extreme form: light absorption becomes bistable. For a given range of intensities of the incident light, both a high absorption state with large plasma concentration and a low absorption state with low plasma concentration can exist.

This kind of optical bistability is observed for different quantum structures: (i) multiple quantum well structures placed inside the intrinsic region of a p–i–n diode connected to an electric circuit with a series resistor [2–5] (SEEDs, i.e. self electro-optical effect devices), (ii) similar structures with an open circuit [6, 7], (iii) multiple quantum well structures placed between charged capacitor plates [8–10] and others [11]. There are two common characteristics for these structures. Firstly, they all show bistable behaviour despite the different character of the relaxation and the transport of electrons and holes. Secondly, all of these structures are layered structures, i.e. extended in two directions, which are perpendicular to the applied field and to the illumination. Thus ignoring carrier motion in the directions perpendicular to the field, each point of the structure could be in either one of the two possible stable states. On the other hand, carrier motion and diffusion on the transversal directions couple the states at different points and eventually produce nonuniform patterns in the electron–hole plasma, as reported recently in experimental [8–10] and theoretical [12] papers. More precisely, these patterns consist of regions with different absorption and electron–hole concentrations of the quasi-neutral plasma, and different configurations of the electrostatic field.

† Temporarily on leave from: Institute of Semiconductor Physics, National Academy of Sciences, Kiev 252650, Ukraine.

‡ To whom all correspondence should be addressed.

0953-8984/98/310539+08$19.50

Under the conventional QCSE in quantum wells, the quantized vertical motion of carriers and their transversal motion are entirely uncoupled. The external field separates electrons and holes and produces a homogeneous charge dipole layer inside the well. If patterns are formed, the vertical and transversal degrees of freedom of the carriers become *strongly coupled*. This leads to the appearance of a complex structure of wave functions and electric charges inside the quantum well layer. In this letter we investigate this structure for different patterns in detail.

Our approach is based upon the consideration of the widely separated characteristic length scales involved in the problem. These include: the well width $2d$, the transversal electron wavelength λ_{dB}, the screening length of the two-dimensional (2D) electron–hole gas l_{sc}, and the ambipolar diffusion length $L_{\mathcal{D}}$, which is expected to be the characteristic length scale of the transversal patterns ($L_{\mathcal{D}} = \sqrt{\mathcal{D}_0 \tau_R}$, where $\mathcal{D}_0$ is a diffusion coefficient and τ_R is the plasma recombination time). For typical experimental conditions, the following relations hold:

$$L_D \gg \lambda_{dB},\ l_{sc},\ d. \tag{1}$$

This allows us to use the following approximations: (i) the total wave functions of the carriers are factorized to the product of the wave functions of the vertical and transversal motion, (ii) the transversal transport of carriers is quasi-classical, (iii) the wave functions of the quantized vertical motion, ψ_e, ψ_h, and the subband energies, ϵ_e, ϵ_h, depend on the transversal coordinates parametrically, and (iv) the redistribution of the electron and hole concentrations is quasi-neutral, $n \approx p$. For simplicity we also assume that the effective masses of both electrons and holes are equal. The basic equations are: Schrödinger equation for electron and hole wave functions in the Hartree approximation, Poisson equation for the electrostatic potential, and drift–diffusion equations for the two-dimensional electron and hole concentrations.

Let us apply an external electric field to a photoexcited single quantum well layer. Introducing the characteristic energy $E_0 = \hbar^2/2md^2$, we will measure subband energies and potential energy in units of E_0, and the electric field in units of E_0/ed. The dimensionless electron and hole concentrations are in units of $\epsilon_0 E_0/e^2 d$, ϵ_0 being the permittivity of the material. Let ζ be the vertical coordinate in units of d and $\boldsymbol{r} = (\xi, \eta)$ be the transversal coordinates in units $L_{\mathcal{D}}$. Using equation (1) we can prove that the dimensionless electrostatic energy can be presented as $v(\xi, \eta, \zeta) = v_0(\zeta; n) + \phi(\boldsymbol{r}) + \mathcal{O}(\boldsymbol{d}/\boldsymbol{L}_{\mathcal{D}})$, with

$$v_0(\zeta; n) = n \int_{-1}^{1} \mathrm{d}\zeta' \mathcal{K}(\zeta, \zeta') \left|\psi_e(\zeta'; n)\right|^2$$

$$\mathcal{K}(\zeta, \zeta') \equiv \frac{1}{2}(|\zeta - \zeta'| - |\zeta + \zeta'|).$$

Here the electron concentration $n(\boldsymbol{r})$ and $\phi(\boldsymbol{r})$ are as yet unknown functions independent of ζ which will be determined later. When the previous scaling and approximations are introduced into the system of coupled Schrödinger–Poisson equations, the resulting problem possesses the following symmetry properties: $v(\zeta; n) = -v(-\zeta; n)$ and $\psi_e(\zeta; n) = \psi_h(-\zeta; n)$. This allows us to obtain wave functions and subbands from the following Schrödinger equation:

$$\frac{\mathrm{d}^2\psi}{\mathrm{d}\zeta^2} + (\epsilon + v_0 - q\zeta)\psi = 0 \tag{2}$$

$$\psi(\pm 1) = 0 \qquad \int_{-1}^{1} |\psi(\zeta; n)|^2 \,\mathrm{d}\zeta = 1$$

where ϵ and ψ depend parametrically on $n(\boldsymbol{r})$ and q is the dimensionless electric field. We obtain for electrons and holes $\psi_e = \psi(\zeta; n)$, $\psi_h = \psi(-\zeta; n)$, respectively. The subband energies are $\epsilon_e(\boldsymbol{r}) = -\phi(\boldsymbol{r}) + \epsilon(\boldsymbol{n}(\boldsymbol{r}))$ and $\epsilon_h(\boldsymbol{r}) = \phi(\boldsymbol{r}) + \epsilon(\boldsymbol{n}(\boldsymbol{r}))$. The solutions of equation (2) were found by means of a variational method. The energy ϵ as a function of the plasma density n for a particular value of the electric field q is presented in figure 1. The parameters used in the calculations are given in table 1. The increase in the electron and hole energies with carrier concentration obviously arises from the screening of the applied field.

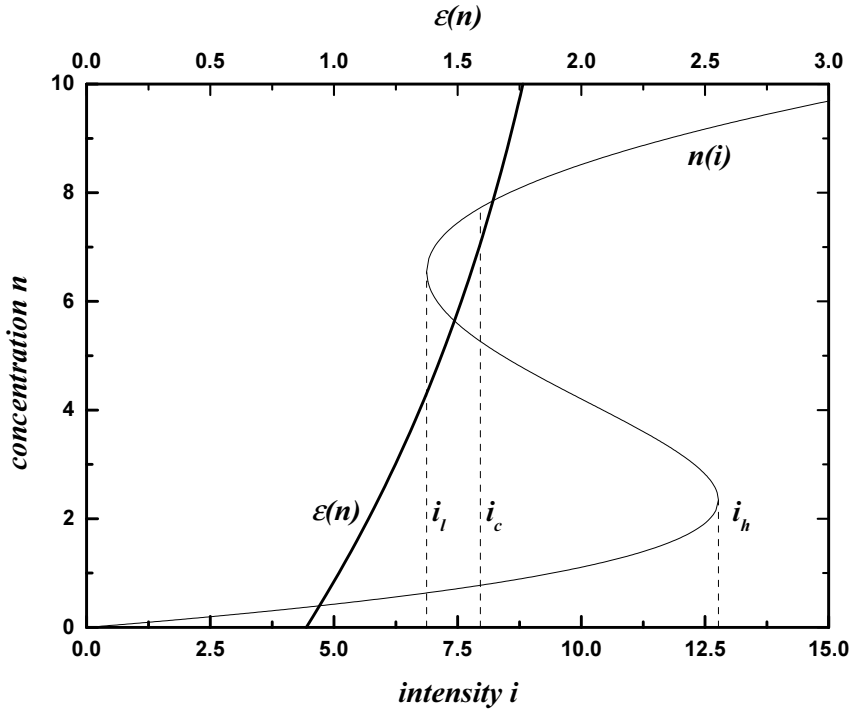

Figure 1. Renormalized energy ϵ (scale on top of the figure) as a function of the plasma concentration n (left axis), and bistable characteristic curve $n(i)$: plasma concentration as function of the incident light intensity i (left and bottom axis).

Table 1. Typical numerical values.

Parameter	Value
E_0 (meV)	5.6
$\mathcal{E}_0$ (kV cm^{-1})	5.6
$\mathcal{N}_0$ (cm^{-2})	4.0×10^{10}
$\mathcal{I}_0/\hbar\omega$ (photons cm^{-2} s^{-1})	8.1×10^{21}

To determine the second contribution to the potential, ϕ, and the electron density, n, we use the drift–diffusion equations written in dimensionless form as

$$\frac{1+\beta}{2\beta}\nabla_{\boldsymbol{r}} \cdot [n\nabla_{\boldsymbol{r}}(\phi - \epsilon(n)) - \alpha(n)\nabla_{\boldsymbol{r}} n] = \mathcal{G} - \mathcal{R}. \tag{3}$$

$$-\frac{1+\beta}{2}\nabla_r \cdot \left[p\nabla_r(\phi+\epsilon(n))+\alpha(n)\nabla_r p\right]=\mathcal{G}-\mathcal{R}. \tag{4}$$

Here $\beta = \mu_p/\mu_n$ is the ratio between the hole and electron mobilities, and we have chosen the diffusion coefficient in the ambipolar diffusion length, $L_{\mathcal{D}} = \sqrt{\mathcal{D}_0\tau_R}$, so that $e\mathcal{D}_0 = 2\beta\mu_n/(1+\beta)$. In these equations, the carriers move on the plane due to the forces $\pm\nabla_r(\phi \mp \epsilon(n))$, for electrons and holes, respectively. $\mu_{n,p}$ are electron and hole mobilities. The second term within the brackets is the diffusion contribution. Note that the potentials v_0 and ϕ generate forces acting on electrons and holes in different ways. In equations (3) and (4), we have defined the function $\alpha(n) = e\mathcal{D}_{n,p}/E_0\mu_{n,p}$, which does not depend on the type of carriers and can be easily found from the Einstein relation. The terms in the right-hand side represent the rates of photo-generation and recombination of the carriers, measured in units of $\epsilon_0 E_0/e^2 d\tau_R$.

In what follows, we restrict ourselves to patterns which depend on a single transversal coordinate, let us say ξ. Subtracting (4) from (3) and using the condition $n \approx p$ we obtain for ϕ:

$$\phi(n) = \frac{1-\beta}{1+\beta}\left(\int^n \frac{\alpha(n)\mathrm{d}n}{n}+\epsilon(n)\right)+\text{constant}. \tag{5}$$

Thus, once $n(\xi)$ is known, we can calculate the electrostatic potential in the QW, $v(\zeta; n)$.

Now we shall specify the generation and recombination rates as: $\mathcal{G}-\mathcal{R} = a(n,q,\omega)i-n$, where $a(n,q,\omega)$ is the dimensionless absorption factor in units of the maximum absorption A_0, i is the light intensity in units $\epsilon_0 E_0\overline{h}\omega/e^2\tau_R A_0 d$, and $\overline{h}\omega$ the photon energy.

Generally, the bistable regimes arise if the absorption factor $a(n,q,\omega)$ is a superlinear function of the plasma concentration and $\mathcal{G}-\mathcal{R}$ has several zeros at fixed q. Our general results do not require specification of $\alpha(n)$, but to obtain numerical results we follow [8–10] and suppose that the absorption is due to exciton generation. These excitons are associated with the two-dimensional electron and hole subbands. A fast exchange between the excitons and the electron–hole states is supposed, so that we can characterize the system by the electron and hole concentrations. In the case of deep QWs and a large exciton radius, the exciton energy E_{ex} follows the positions of the electron and hole subbands. Assuming a Lorentz shape of the absorption factor as function of the photon energy, we can write:

$$a(n,q,\omega) = \frac{\Lambda^2}{(\epsilon(n,q)-\Delta)^2+\Lambda^2} \tag{6}$$

where $\Delta = -(E_g - E_{ex} - \overline{h}\omega)/2E_0$, is the detuning of the photon energy, and Λ is the dimensionless bandwidth in units $2E_0$. It is obvious that for the shape of the absorption (6), the right-hand side of equations (3) and (4) can have more than one solution at a detuning $\Delta(\omega) > \epsilon(0,q)$.

Now we can obtain the final 'diffusion-like' equation for n from equations (3)–(5)

$$-\frac{\partial}{\partial\xi}\left\{\mathcal{D}(n,q)\frac{\partial n}{\partial\xi}\right\} = a(n,q)i - n \equiv R(n,q,\omega,i) \tag{7}$$

where $\mathcal{D}$ is a function of the concentration n and the electric field q: $\mathcal{D}(n,q) \equiv \alpha(n) + n\frac{\partial\epsilon(n,q)}{\partial n}$. It is important to notice that the 'diffusion coefficient' $\mathcal{D}(n,q)$ is strictly positive for all $n \geqslant 0$.

The condition $R(n,q,\omega,i) = 0$ gives transversally uniform solutions. It can be shown that in equation (6) there are intervals of intensities and electric fields with *three* branches of uniform solutions $n = n(i,q)$: low absorption branch (low concentration $n_l(i)$), high absorption branch (high concentration $n_h(i)$) and the middle branch. The latter is unstable.

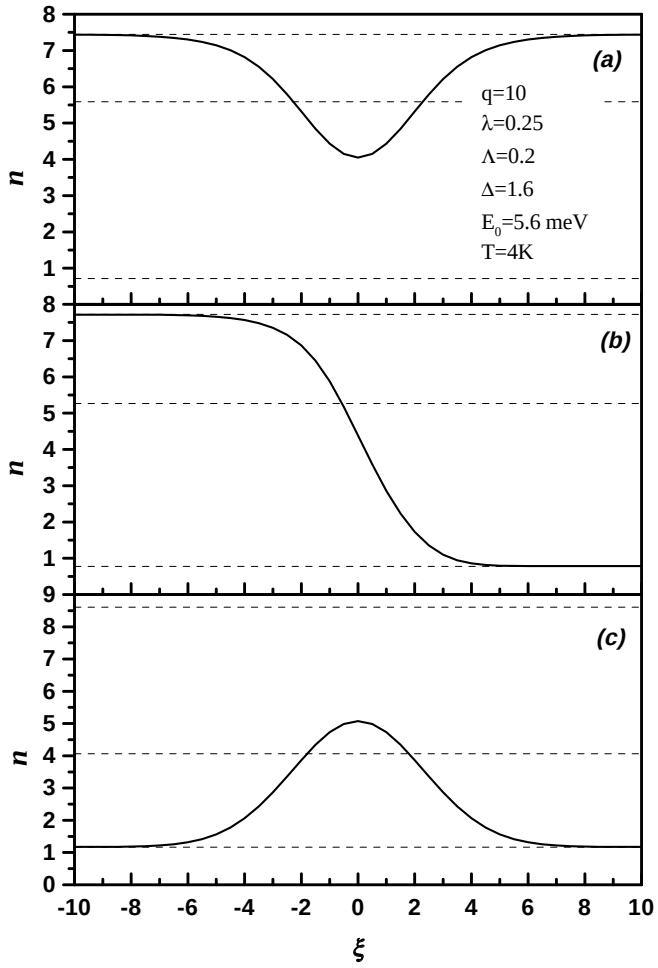

Figure 2. Three basic types of pattern for infinite transversal extension of the QW layer. Considering the phase portrait of equation (7); (a) corresponds to the homoclinic orbit when $i_l < i < i_c$, (b) corresponds to a heteroclinic orbit when $i = i_c$, and (c) corresponds to the homoclinic orbit when $i_c < k < i_h$. Parameter values are shown in the body of the figure.

In figure 1 we present these branches calculated for particular parameters of table 1. The bistable regime occurs in the interval $i_l < i < i_h$.

Nonuniform solutions of equation (7) can be found in an implicit form. A first integral is

$$\frac{1}{2}\mathcal{D}^2(n)\left(\frac{\mathrm{d}n}{\mathrm{d}\xi}\right)^2 + U(n,i) = C_1 \tag{8}$$

$$U(n,i) = \int_{n_l}^{n} \mathrm{d}n'\ R(n',i)\mathcal{D}(n').$$

Then the solutions are given by:

$$\pm\int^{n} \frac{\mathcal{D}(n')\mathrm{d}n'}{\sqrt{2(C_1 - U(n',i))}} = \xi + C_2 \tag{9}$$

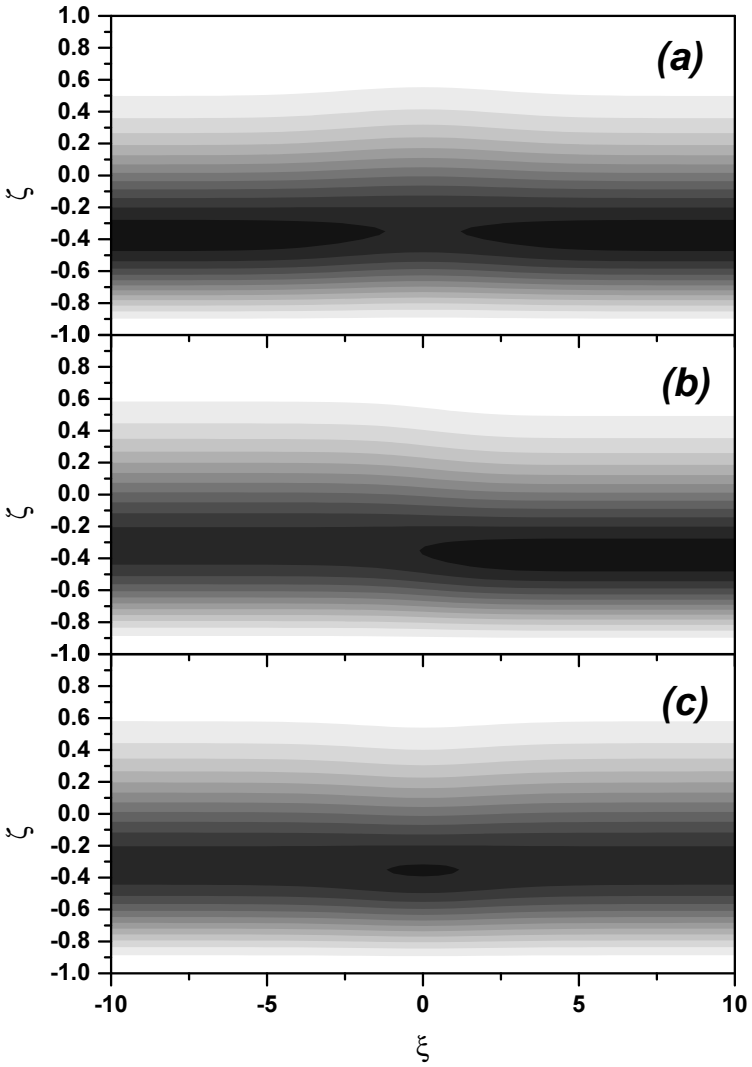

Figure 3. Distribution of the square of the electrons wave function $|\psi_e|^2$ for the three basic patterns portrayed in figure 2.

where C_1 and C_2 are constants.

Let us suppose that the quantum well layer is infinite in the ξ direction. Then possible nonuniform solutions $n(\xi)$ should tend to the stable fixed points $n_l(i)$ or $n_h(i)$ as $\xi \to \pm\infty$. There are three types of such nonuniform solutions. To classify them we shall introduce a critical value of the intensity, i_c, which solves the equation

$$U(n_h(i_c), i_c) = 0. \tag{10}$$

The nonuniform solutions are homoclinic and heteroclinic orbits in the phase plane defined by equation (7): (i) *anti-soliton-like* patterns having a single minimum and such that $n(\xi) \to n_h(i)$ as $|\xi| \to \infty$ (if $i_l < i < i_c$), (ii) *kink-like* patterns (if $i = i_c$), and (iii) *soliton-like* patterns having a single maximum and such that $n(\xi) \to n_l(i)$ as $|\xi| \to \infty$ (if $i_c < i < i_h$). These patterns are illustrated in figure 2. Besides these patterns, we found

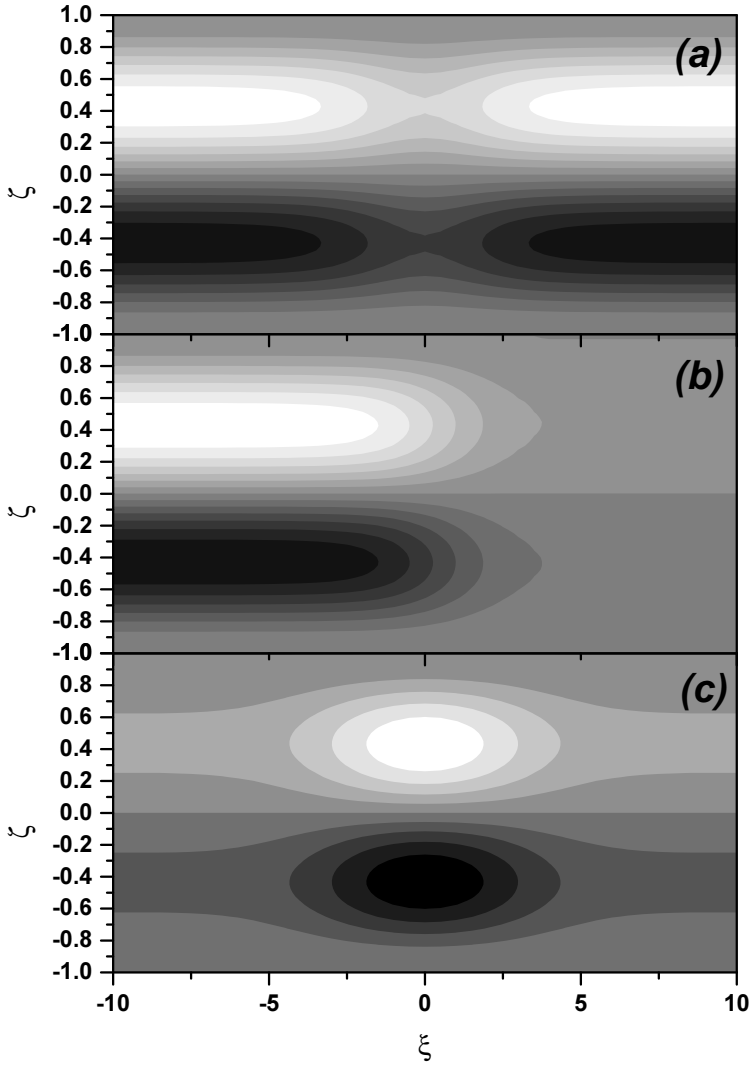

Figure 4. Electric charge distribution for the three basic patterns portrayed in figure 2.

an infinite number of periodic solutions. For a given i, their amplitudes vary from zero to $(n_h(i) - n_l(i))$.

Now we consider the three basic patterns listed above. In figure 3 we present density plots of the square of the electron wave functions ($|\psi_e|^2$) inside the quantum well layer under these conditions. The breaking of the transversal translation symmetry can be seen clearly: the carrier wave functions become dependent on the transversal coordinate and are different for each pattern. The wave function distributions are symmetric with respect to the centre of soliton and anti-soliton patterns, whilst the kink-like pattern has an asymmetric wave function distribution. These wave function distributions are due to different screening of the external field in different patterns. For example the field of the soliton-like pattern is considerably screened in the central region by the excess of electrons and holes. There the subband energies ϵ_e, ϵ_h are higher (see figure 1) and the wave function becomes flatter

and uniformly distributed across the quantum well layer (figure 3(c)). All these features correspond to local partial suppression of the QCSE. In contrast, the QCSE is enhanced in the central part of the anti-soliton pattern (figure 3(a)).

Figure 4 depicts the electric charge distributions

$$\rho(\xi, \zeta) = n(\xi)\left(|\psi_h(\zeta|\xi)|^2 - |\psi_e(\zeta|\xi)|^2\right)$$

for the same basic patterns. The central horizontal line at $\zeta = 0$ separates half of the QW layer with a negative charge ($\zeta > 0$) from that with a positive charge ($\zeta < 0$). Notice that instead of a transversally uniform dipole layer we obtain a complex distribution of the electric charge, which adopts the form of a nonuniform dipole layer inside the QW. In the case of the soliton-like pattern (figure 4(c)), there is an excess of carriers in the central region of the pattern. It is there that the dipole strength is maximal. For the anti-soliton pattern (figure 4(a)), two symmetric regions depleted of electrons and holes appear in the central part of the QW. Figure 4(b) shows the charge configuration in the transition region between the states with high and low concentration of a kink-like pattern.

In conclusion, we have studied pattern formation under the QCSE, and found different patterns with a complex structure, of the electron and hole wave functions and of the electric charge inside the QW layer. The results obtained indicate the breaking of the transversal invariance, which can lead to a set of new optical effects and transport phenomena. These include changes in the selection rules for optical transitions, patterning of the transmitted light intensity, anisotropy of the conductivity of two-dimensional electron–hole plasma, etc.

We are indebted to the Dirección General de Enseñanza Superior (Spanish Ministry of Education) for sabbatical support (VAK) and for financial support through grant PB94-0375. One of us (CAV) acknowledges the support of the Fundación General de la Universidad Carlos III de Madrid.

References

[1] Miller D A B, Chemla D S, Damen T C, Gossard A C, Weigmann W, Wood T H and Burrus C A 1984 *Phys. Rev. Lett.* **53** 2173

[2] Miller D A B, Chemla D S, Damen T C, Wood T H, Burrus C A, Gossard A C and Wiegmann W 1985 *IEEE J. Quantum Electron.* **21** 1462

[3] Schmitt-Rink S, Chemla D S and Miller D A B 1989 *Adv. Phys.* **38** 89–188

[4] Lentine A L, Hinton H S, Miller D A B, Henry J E, Cunnningham J E and Chirovski L M F 1989 *IEEE J. Quantum Electron.* **25** 1928

[5] Miller D A B 1990 *Opt. Quantum Electron.* **22** S-61

[6] Abe Y and Tokuda Y 1993 *Appl. Phys. Lett.* **63** 3259

[7] Couturier J, Voisin P and Harmand J C 1994 *Appl. Phys. Lett.* **64** 742
Couturier J, Voisin P and Harmand J C 1993 *J. Physique* **3** 253
Couturier J, Voisin P and Harmand J C 1995 *Semicond. Sci. Technol.* **10** 881

[8] Merlin R 1989 in *Spectroscopy of Semiconductor Microstructures*, *NATO Series B* vol 206 pp 347

[9] Merlin R, Mestres N, McKiernan A, Oh J and Bhattacharya P K 1990 *Surf. Sci.* **228** 88-91

[10] Merlin R and Kessler D A 1990 *Phys. Rev.* B **41** 9953

[11] Double and triple asymmetric quantum wells are close analogues of conventional heterostructures showing the QCSE. For them, the built-in asymmetric potential profile plays the same role as the external field, and illumination gives rise to a redistribution of the electric charge, a change of the effective potential and bistability, see
Trezza J A, Larson M C, Lord S M and Harris Jr S J 1993 *J. Appl. Phys.* **74** 1972
Scandalo S and Tassone F 1992 *Phys. Status Solidi* b **173** 453

[12] Bonilla L L, Kochelap V A, Sokolov V N and Velasco C A 1997 *Phys. Status Solidi* b **204** 559–62